



**HAL**  
open science

# Bond Graph Model of a mechanically Pumped Biphasic Loop (MPBL)

Mohamed Kebdani, Geneviève Dauphin-Tanguy, Antoine Dazin, Patrick Dupont

► **To cite this version:**

Mohamed Kebdani, Geneviève Dauphin-Tanguy, Antoine Dazin, Patrick Dupont. Bond Graph Model of a mechanically Pumped Biphasic Loop (MPBL). 23th Mediterranean Conference on Control and Automation (MED, Jun 2015, Torremolinos, Spain. pp.301 - 329, 10.1109/MED.2015.7158789 . hal-01435310

**HAL Id: hal-01435310**

**<https://hal.science/hal-01435310>**

Submitted on 20 Jan 2017

**HAL** is a multi-disciplinary open access archive for the deposit and dissemination of scientific research documents, whether they are published or not. The documents may come from teaching and research institutions in France or abroad, or from public or private research centers.

L'archive ouverte pluridisciplinaire **HAL**, est destinée au dépôt et à la diffusion de documents scientifiques de niveau recherche, publiés ou non, émanant des établissements d'enseignement et de recherche français ou étrangers, des laboratoires publics ou privés.

# Bond Graph Model of a mechanically Pumped Biphasic Loop. (MPBL).

M. Kebdani\*, G. Dauphin-Tanguy\*, A. Dazin\*\*, P. Dupont\*\*\*.

\* Ecole Centrale de Lille/ CRISTAL UMR CNRS 9189, CS 20048, 59651 Villeneuve d'Ascq. France.  
[mohamed.kebdani@ec-lille.fr](mailto:mohamed.kebdani@ec-lille.fr); [genevieve.dauphin-tanguy@ec-lille.fr](mailto:genevieve.dauphin-tanguy@ec-lille.fr).

\*\* Arts et Métiers Paris Tech/ LML UMR CNRS 8107, Boulevard Louis XIV, 59000 Lille. France.  
[antoine.dazin@ensam.eu](mailto:antoine.dazin@ensam.eu).

\*\*\* Ecole Centrale de Lille/LML UMR CNRS 8107, CS 20048, 59651 Villeneuve d'Ascq. France.  
[patrick.dupont@ec-lille.fr](mailto:patrick.dupont@ec-lille.fr).

**Abstract** - The MPBL is an effective technology in terms of heat flow transport capacity: 10 MW.m, [2], with high level adaptability. A bond graph model of such a system is proposed in this paper. The model is dynamic, qualitative, configurable and pays particular attention to the dynamic of the transient regime. It aims at being a tool dedicated to designing the different components of a MPBL. It is also used for a physical analysis of the system in different operating conditions.

**Keywords:** Bond Graph; Biphasic; dynamic; Systems; Evaporator; cooling.

## I. INTRODUCTION

An electronic module implanted in embedded systems generates heat flows that require evacuation. For example the limit junction temperature of a silicon chip is 125 ° C; if it is exceeded a risk of malfunction is considered.

Volume density of the power dissipated by Joule effect in a converter is quadrupled every four years, providing values that could reach 100 w/cm<sup>3</sup> for the arrival of 2020. Serin, V. [10]. The cooling of electronic devices based only on exchanges by natural convection is designated to low power. Indeed, the apparent heat transfer coefficient remains low: 3-15W.m<sup>-2</sup>.K<sup>-1</sup>. Furthermore, the finned radiators have apparent exchange coefficients up to 300W.m<sup>-2</sup>.K<sup>-1</sup>.

For higher power, fluids loops are more adapted. These fluidic systems can be classified as follows:

**i/ Mechanically Pumped Fluid Loop: MPFL.** The loop is screwed on the circuit support. Inside the loop, a single phase refrigerant liquid is pushed by a pump. It is a forced convection whose apparent coefficient of heat exchange can reach 10<sup>5</sup>W.m<sup>-2</sup>.K<sup>-1</sup>. The fluid is used to extract heat at the electronic component and transport it to a cold source.

**ii/ Capillary Pumped Fluid CPF,** which have been originally developed in the seventies, in the context of space applications. This system is based on the use of the latent heat of a fluid and is potentially able to evacuate important quantities of heat flows. The refrigerant movement is natural and obtained by capillary effect. CPF class is divided into two sub-categories developed in parallel. In the United States: CPL (Capillary Pumped Loop), developed by Stenger in 1966, Muraoka [5] in Russia, the LHP (Loop Heat Pipe), designed by Gerasimov and Maydanik 1975, Wang et al. [12]. The only difference between the two architectures is the positioning of the tank. CPF are distinguished by: transportation capacity powers ranging from 500W to 24000W, architectural flexibility and phases separation

eliminating every phasic interactions.

## iii/ Mechanically Pumped Biphasic Loop (MPBL).

### ➤ MPBL components.

The principle of this system is quite similar to the previous one, but the fluid, trapped inside the loop, is moved by a pump. This allows greater flow rates and consequently greater heat flow transfer.

The main components of MPBL are the following ones:

#### a. The evaporator.

The heat source propagates heat flow, by conduction and convection, toward the fluid. This one extracts the flow by a phenomenon of vaporization, and evacuates it to the condenser. An evaporator is place of strongly and complex coupled thermal-hydraulics phenomena: evaporation, change of state, two-phase flow, dynamic movement of the evaporation front, evaporation rate...

#### b. The condenser.

Because of the heat exchange realized inside the condenser between the fluid source and a secondary refrigerant, the fluid condenses and releases the stored energy. Also, the condenser under cools the refrigerant to avoid cavitations.

#### c. The Tank and the pipes.

The thermo hydraulic control of the entire loop is possible through a thermal regulation of the fluid in the tank. This regulation allows the control of the pressure at the liquid / vapor interface in the tank. Knowing the losses, evaporation pressure is deduced. In general, the losses are small: it means that the pressure in the tank represents a reference for the whole system performance. In addition, the tank must be able to supply the loop with the liquid quantity needed for a good functioning, regardless whatever is the regime.

#### e. The pump.

The mechanical pump is located upstream of the evaporator (Fig. 6), the pump motor is powered by an external voltage source. Currently, we are in a step of feasibility study and performance evaluation of such a device.

### ➤ Existing Numerical models.

Few papers in the literature deal with MPBL components bond graph (BG) modeling. A BG model detailed of a condenser is proposed by Medjaher. and al. [3]. The work is

about the functioning of the heat exchanger, and presents a physical model formulation of the problem with a BG whose simulation results are consistent with the experimental. The work of B. Bouamama and al. [7] fits along the same lines of modeling a steam condenser with BG. The scientific literature shows few studies that provide numerical models of fluid loops, and even less of two-phase loops. However, we can cite the work of B. Ould Bouamama and al. [6] studying the complex behavior of a steam generator consisting of a condenser, steam accumulator and pipes. The authors bring forward a comprehensive model BG of the installation. Another numerical modeling work is proposed by Platell and al. [8] where they present a non-stationary model of CPL. Also in the same vein, Lachasagne [2] proposes an analytical model dedicated to CPL and based on an original modeling approach called nodal.

As to MPBL, at our knowledge, no modeling work of the complete loop has been published at present time.

The work presented in this paper is intended to contribute to the theoretical study of a MPBL with a specific attention on the phase changes in the heat exchanger. Modeling and simulation are performed using the software 20sim by adopting the BG methodology (Thoma [11], and Mukherjee [4]). It is used to show up the power exchanges in a multidisciplinary dynamic system (mechanical, electrical, hydraulic, thermal ...) based on the principle of power conservation and causality property [1]. The control of mass and enthalpy balance is capital and must be completed for each component of the loop. The notion of junction "0 and its dual 1" facilitates the representation of mass and enthalpy conservation.

The purpose is to be able to predict the behavior of the loop in transient and steady operations and consequently to provide a pertinent tool for the design of such loops.

The results of the model are also used to analyze the physical behavior of the system during several operating conditions.

## II. BOND GRAPH MODEL.

### II.1. Generalized variables used in the model.

Two complementary pairs of variables, involved in the calculation of the transferred powers are defined in the sense of the bond graph methodology as:

**For the hydraulic part,** the effort variable is the pressure in the loop and the flow variable is the mass flow rate. The resulting model is a "pseudo" bond graph. The choice of the mass flow rate is justified by the fact that it is more adapted than volume flow rate for the formulation of the continuity equation in the case of a biphasic flow, in which the density is varying with time.

**For the thermal part:** the effort variable is the temperature and the flow variable is enthalpy flow. Enthalpy flow is preferred to entropy flow because energy balance is naturally written with this first variable. Furthermore, the choice of these variables allows constructing the thermodynamic functions of refrigerant used and calculating other system variables.

## II.2. BG used to model a MPBL.

### II.2.1. Model assumptions.

The refrigerant used for the simulation is water; its thermo physical features are extracted from Schmidt [9]. The model is based on the following assumptions:  
 The liquid flow is considered one-dimensional.  
 Hydraulic inertia of fluid is not taken into account.  
 Pressure is imposed in the upper part of the tank.  
 The liquid-vapor mixture has uniform pressure.  
 All pipes are perfectly adiabatic.  
 There is no fluid storage in the pipes.

### II.2.2. Word Bond Graph model of the loop.

The Word Bond Graph model is proposed Fig.6 in which we find the loop components described in the introduction.

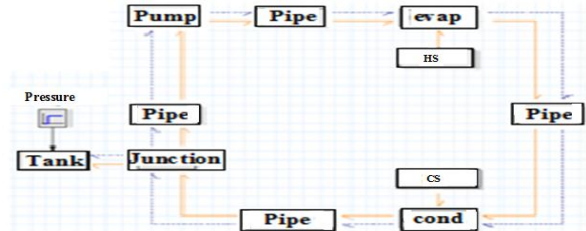


Fig.6: Word Bond Graph of a MPBL.

### II.2.3. Detailed Bond Graph of the evaporator.

The global model Fig 7 of the evaporator is composed of three sub models:

- Sub-model 1:** Purely Liquid region of the evaporator. The model used is a passive element multiport RC, where both hydro and thermal energies are coupled: R describes the energy dissipation due to load losses. C expresses the heat storage in the thermal part.
- Sub-model 2:** two-phase mixing region. The model used is a passive two-port element C, storing mass in the hydraulic part and heat in the thermal part.
- Sub-model 3:** surface between the two previous regions. A multiport element R provides coupling between the two areas, and describes the phase change.

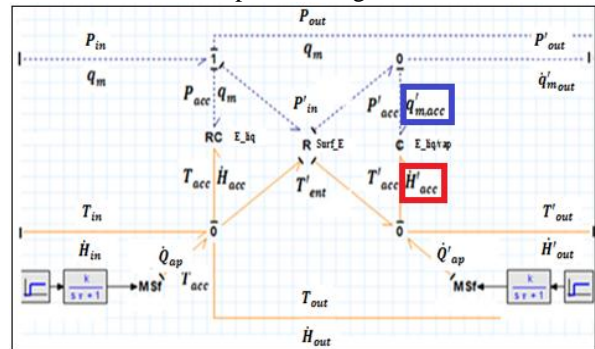


Fig.7: BG Model of the evaporator.

#### a. Energy equation

The general expression of the enthalpy flow is:

$$\dot{H} = q_m * \left( u + \frac{P}{\rho} + \frac{\rho * v^2}{2} \right) = q_m * \left( h + \frac{\rho * v^2}{2} \right)$$

At low speeds  $v$ , the kinetic energy:  $\frac{\rho * v^2}{2}$  is neglected, and

$$\dot{H} = q_m * h = q_m * C_p * T.$$

Two operating conditions are modeled:

**Case 1: mono-phasic fluid in the whole evaporator:**

The blocks R and C are disabled and do not exchange power. It is the RC submodel which represents the evaporator behavior in the liquid state, we have:

$$\begin{aligned} P_{in} &= P_{acc} + P_{out} & 1 \\ T_{out} &= T_{in} = T_{acc} & 2 \\ \dot{H}_{acc} &= \dot{H}_{in} + \dot{Q}_{ap} - \dot{H}_{out} & 3 \end{aligned}$$

**Case 2: The fluid is biphasic (liquid/vapor):**

The submodel RC of Fig.7 represents the liquid part of the evaporator while models R and C describe the physical phenomena of the liquid in its two-phase state:

$$\begin{aligned} P'_{out} &= P'_{in} = P'_{acc} & 4 \\ q'_{m,acc} &= q_m - q'_{m,out} & 5 \\ T'_{out} &= T'_{in} = T'_{acc} & 6 \\ \dot{H}'_{acc} &= \dot{H}'_{in} - \dot{H}'_{out} + \dot{Q}'_{ap} & 7 \end{aligned}$$

**b. Equations associated to the evaporator model.**

➤ **Element RC modeling the liquid part.**

➤ **Hydraulic part:**

Fluid mass in the evaporator:

$$m0 = \rho_{liq} * V_{evap} \quad 8$$

Initial enthalpy :

$$H_0 = m_0 * C_p * T_0 \quad 9$$

➤ **Thermal part :**

$$\begin{aligned} H_{evap} &= \int \dot{H}'_{acc} dt + H_0 & 10 \\ T_{evap} &= \frac{H_{evap}}{m_0 * C_p} \end{aligned}$$

➤ **Element C modeling the mixing part.**

➤ **State change indicator.**

Initially, the fluid is mono-phasic. After heat source activation, its temperature rises gradually to reach the saturation value. The fluid becomes biphasic. To specify this state change, and then be able to activate the model C of the evaporator, a Boolean indicator is introduced. This indicator noted ( $ind_E$ ) is built according to the following logic:

First, the saturation temperature corresponding to the pressure in the evaporator is calculated, by applying a polynomial approximation to the results provided by the thermodynamic tables:

$$T_{sat} = \sum_{i=0}^{i=6} p_i * P^i \quad 11$$

If the liquid temperature  $T_{evap}$  is greater than  $T_{sat}$ , the fluid is biphasic and we take:  $ind_E = 1$ , otherwise  $ind_E = 0$ .

➤ **Hydraulic and heat balances inside the evaporator.**

Conservation laws monitoring an evaporator operating in biphasic regime with phase change are:

Mass balance:

$$q'_{m,acc} = q_m - q'_{m,out} \quad 12$$

Energy balance :

$$\dot{H}'_{acc} = \dot{H}'_{in} - \dot{H}'_{out} + \dot{Q}_{ap} \quad 13$$

Heat flow entering into the evaporator:

$$\dot{H}_{in\ evap} = q_m * C_p * T_{sat} \quad 14$$

Heat flow leaving the evaporator:

$$\dot{H}'_{out} = q'_{m,out} * C_p * T_{acc} \quad 15$$

Phase change equation:

$$\dot{H}_{in\ evap} - \dot{H}'_{out} = L_v * (q_m - q'_{m,out}) \quad 16$$

➤ **Determination of the mixture pressure " $P_{evap}$ "**

The heat flow  $\dot{H}'_{acc}$  and the mass flow  $q'_{m,acc}$  (Fig.7) are calculated (eq. 5 and 7), and after integration (eq. 17 and 18) the specific enthalpy  $h$  (eq.19) and specific volume  $v$  (eq.20) are obtained. From these two values and the enthalpy diagram is raised the mixture pressure  $P_{evap}$  (eq.23).

The mass of liquid in the evaporator is:

$$m_{evap} = \int q'_{m,acc} dt + m_0 \quad 17$$

The enthalpy in the evaporator is:

$$H_{evap} = \int \dot{H}'_{acc} dt + H_0 \quad 18$$

From these values and the evaporator volume ( $V_{evap}$ ) we can obtain the specific enthalpy and volume:

$$h = \frac{H_{evap}}{m_{evap}} \quad 19$$

$$v = \frac{V_{evap}}{m_{evap}} \quad 20$$

Furthermore, the specific volume of the mixture is:

$$v = v''(P) * X + v'(P) * (1 - X) \quad 21$$

And the specific enthalpy of the mixture is:

$$h = h''(P) * X + h'(P) * (1 - X) \quad 22$$

After some arrangements we get the 12<sup>th</sup> degree polynomial where the unknown variable is the pressure  $P_{evap}$ :

All functions:  $h', h'', v', v''$  are some known thermo- dynamics equations depending on pressure  $P_{evap}$ .

$$v * [h'' - h'] - v'' * [h - h'] - v' * [h'' - h] = 0. \quad 23$$

To calculate the pressure of the mixture, 20sim sends at each time, to Matlab the specific enthalpy  $h$  and the specific volume  $v$ . Using these two values Matlab solves the polynomial (eq. 23), and calculates the adequate root.

➤ **Vapor quality " $X$ ".**

The vapor quality expression is:

$$X = \frac{v - v'(P_{evap})}{v''(P_{evap}) - v'(P_{evap})} \quad 24$$

**II.2.4. Model of the other elements of the MPBL.**

At the present study, the pump is considered as a flow rate source, the tank is modeled as a source of pressure. Pipes

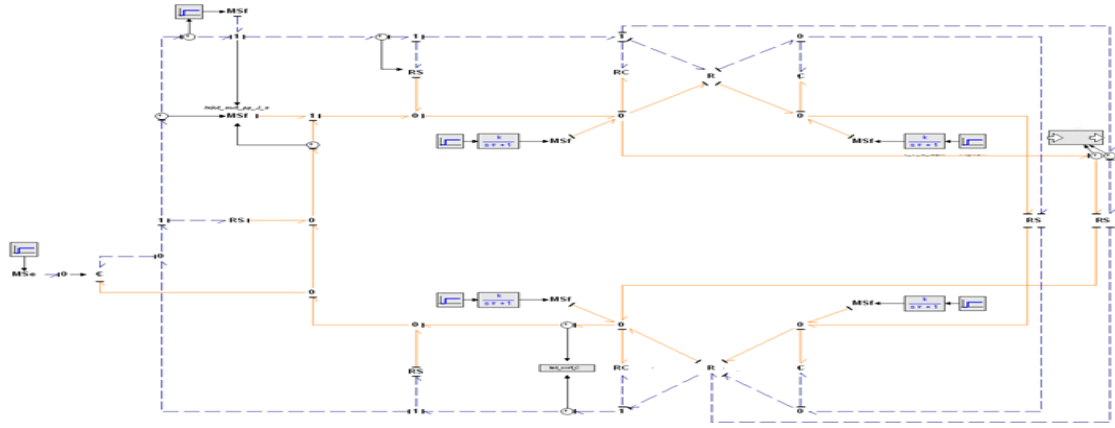


Fig 8: General BG model of a MPBL.

modelise load losses (elements R) and fluid heating caused by frictions forces (elements S). At last, the condenser model is quite similar to the evaporator model (Fig 8).

### III. RESULTS AND ANALYSIS.

Component		Value	Unit
Evaporator volume		$3 * 10^{-5}$	$m^3$
Condenser volume		$4 * 10^{-5}$	$m^3$
Tank volume		$9 * 10^{-9}$	$m^3$
Pipe length	Evap-Cond	0.388	$m$
	Cond- tank	0.225	$m$
	tank -pump	0.26	$m$
Pipe diameter	Pump-evap	0.14	$m$
		0.00334	$m$

Table.1. Geometrical dimensions of MPBL components.

#### III.1. Cold and hot thermal power sources disabled.

##### Simulation conditions:

Injected power = 0 W; Dissipated power = 0W.

Initial pressure =1.3 bar; initial temperature = 310K

Mass flow rate =  $5 \text{ cm}^3/\text{s}$ .

The temperatures in the evaporator (blue curve) and the condenser (orange curve) starts from the initial value 310K and increase very slightly, a few hundredths of a degree. This temperature increase is due to fluid friction.

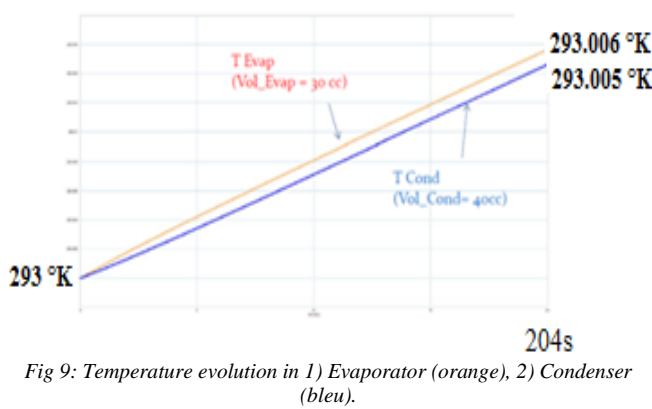


Fig 9: Temperature evolution in 1) Evaporator (orange), 2) Condenser (bleu).

#### III.2. Dynamic study of liquid phase thermal behavior.

In pure monophasic operating conditions, the MPBL is mainly a place of thermal process. In this section a dynamic study of the thermal behavior is proposed.

To perform an analytical study of temperatures in the exchangers, a simplified analogous electrical model of the MPBL (Fig.10 (a)) and its BG (Fig.10 (b)) are proposed, to enable better comprehension of the real MPBL behavior.

Thermal flow sources are analogous to current sources "Cold source" and "Hot source" (Fig.10 (a)). The evaporator and condenser are reduced to capacitors noted successively:  $C_{evap}$  and  $C_{cond}$ . Pipes are assimilated to an electrical resistor.

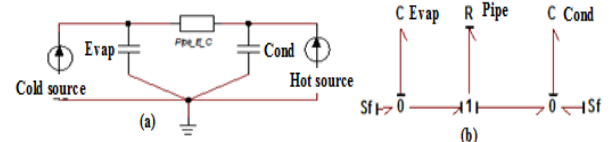


Fig.10. (a) Equivalent electrical model of the MPBL, (b) BG of the equivalent MPBL model.

where:  $C_{evap} = C_p \cdot m_{liq\_evap}$ ,  $C_{cond} = C_p \cdot m_{liq\_cond}$ ,  $R_{pipe} = \frac{1}{C_p \cdot q_{m0}}$

The different parameters are supposed to be constant and not temperature dependent. The model is linear.

The differential state equation of the equivalent model is (eq.25):

$$\begin{bmatrix} \dot{T}_{evap} \\ \dot{T}_{cond} \end{bmatrix}_x = \underbrace{\begin{bmatrix} \frac{1}{RC_{evap}} & \frac{1}{RC_{evap}} \\ \frac{1}{RC_{cond}} & -\frac{1}{RC_{cond}} \end{bmatrix}}_A \begin{bmatrix} T_{evap} \\ T_{cond} \end{bmatrix}_x + \underbrace{\begin{bmatrix} \frac{1}{C_{evap}} & 0 \\ 0 & \frac{1}{C_{cond}} \end{bmatrix}}_B \begin{bmatrix} P_{ch} \\ P_{fr} \end{bmatrix}_u$$

With Initial condition:  $x_0 = \begin{bmatrix} T_{0\_evap} \\ T_{0\_cond} \end{bmatrix}$ .

We can remark that:  $\det A = 0$ , which means that the exchangers have an integrator-type behavior. The deduced transfer matrix is thus (eq.26):

$$\begin{bmatrix} T_{evap}(s) \\ T_{cond}(s) \end{bmatrix} = \frac{1}{s(s + \frac{1}{\tau_{evap}} + \frac{1}{\tau_{cond}})} \begin{bmatrix} (s + \frac{1}{\tau_{cond}}) & \frac{1}{\tau_{evap}} \\ \frac{1}{\tau_{cond}} & (s + \frac{1}{\tau_{evap}}) \end{bmatrix} \begin{bmatrix} \frac{1}{C_{evap}} & 0 \\ 0 & \frac{1}{C_{cond}} \end{bmatrix} \begin{bmatrix} P_{ch} \\ P_{fr} \end{bmatrix} + \begin{bmatrix} T_{0\_evap} \\ T_{0\_cond} \end{bmatrix}$$

with:  $\tau_{evap} = RC_{evap}$ ,  $\tau_{cond} = RC_{cond}$

#### ➤ Analysis case n°1:

Hot source  $P_{HS} = 0W$ , Cold source  $P_{CS} = 0W$ .

The initial temperatures are different ( $293^\circ K / 313^\circ K$ ).

The stabilized regime is given by (eq.27 and 28):



$$T_{evap}(\infty) = T_{cond}(\infty) = \frac{1}{\left(\frac{1}{\tau_{evap}} + \frac{1}{\tau_{cond}}\right)} \left( \frac{1}{\tau_{cond}} T_{0\_evap} + \frac{1}{\tau_{evap}} T_{0\_cond} \right)$$

$$T_{evap}(\infty) = T_{cond}(\infty) = \frac{m_{liq\_evap} T_{0\_evap} + m_{liq\_cond} T_{0\_cond}}{(m_{liq\_evap} + m_{liq\_cond})}$$

The permanent regime behavior depends only on liquid masses and initial temperatures in exchangers.

### ➤ Analysis case n°2:

Hot source  $P_{HS}=200W$ , Cold source  $P_{CS}=0W$ .  
The temperatures are initially the same (293 °K).  
According to the system equation (Eq. 26) we have:

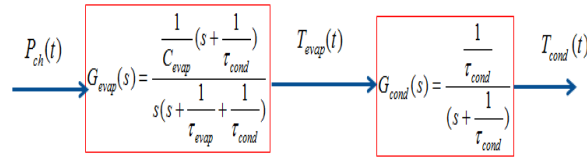


Fig.11. Transfer functions of the equivalent model.

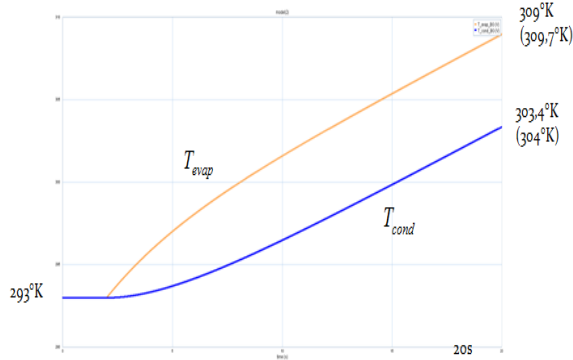


Fig.12. Temperature evolution of both electrical model and MPBL.

The graph 12 shows very similar temperatures evolution in both, electrical and MPBL model. The difference in the transient evolution of  $T_{evap}$  and  $T_{cond}$  is due to the influence of the filter  $G_{cond}(s)$  whose expression is shown in Fig.11.

### III.3. Cold and hot sources activated, no changing phase.

A second simulation, injected powers have opposite signs but same amplitude ( $P_{HS}=-P_{CS}=-P_{cho}$ ) is now considered. The temperatures are initially the same (293°K). A simple development of (Eq. 26) allows writing:

$$T_{evap}(s) = \frac{P_{ch0}(s)}{C_{evap} \left( s + \frac{1}{\tau_{evap}} + \frac{1}{\tau_{cond}} \right)} + \frac{\left( s + \frac{1}{\tau_{cond}} \right) T_{0\_evap} + \frac{1}{\tau_{evap}} T_{0\_cond}}{s \left( s + \frac{1}{\tau_{evap}} + \frac{1}{\tau_{cond}} \right)}$$

$$T_{cond}(s) = - \frac{P_{ch0}(s)}{C_{cond} \left( s + \frac{1}{\tau_{evap}} + \frac{1}{\tau_{cond}} \right)} + \frac{\frac{1}{\tau_{cond}} T_{0\_evap} \left( s + \frac{1}{\tau_{evap}} \right) T_{0\_cond}}{s \left( s + \frac{1}{\tau_{evap}} + \frac{1}{\tau_{cond}} \right)}$$

First of all, we can remark that integrator behavior has been cancelled. It is possible to predict the stabilized regime:

$$T_{evap}(\infty) = \frac{P_{ch0}}{C_{evap} \left( \frac{1}{\tau_{evap}} + \frac{1}{\tau_{cond}} \right)} + T_0(\infty)$$

$$T_{cond}(\infty) = - \frac{P_{ch0}}{C_{cond} \left( \frac{1}{\tau_{evap}} + \frac{1}{\tau_{cond}} \right)} + T_0(\infty)$$

with:

$$T_0(\infty) = \frac{\left( \frac{1}{\tau_{cond}} \right) T_{0\_evap} + \frac{1}{\tau_{evap}} T_{0\_cond}}{\left( \frac{1}{\tau_{evap}} + \frac{1}{\tau_{cond}} \right)}$$

This means that final temperature in the evaporator is different from the one in the condenser (fig.13).

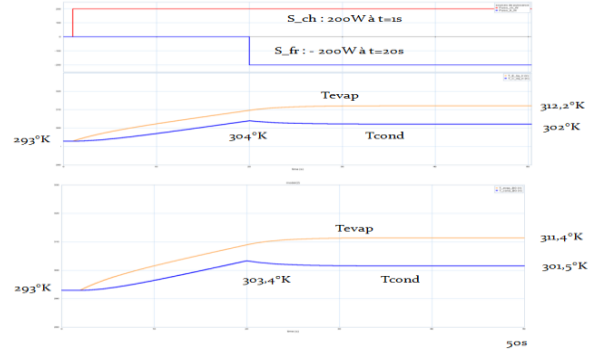


Fig.13. Applied power. MPBL Model. Equivalent Electrical Model

In this case also, the graph 13 shows very similar temperatures evolution in both, electrical and MPBL model.

### III.4. Phase change.

A final simulation with phases changes in the heat exchangers is now described and analyzed:

#### simulation conditions:

$P_{HS}=2000W$  at  $t=1s$ .  $P_{CS}=-2000W$  at  $t=15s$ .

$P_0=1.3$  bar;  $T_0=293$  K;  $q_m=5$  cm<sup>3</sup>/s.

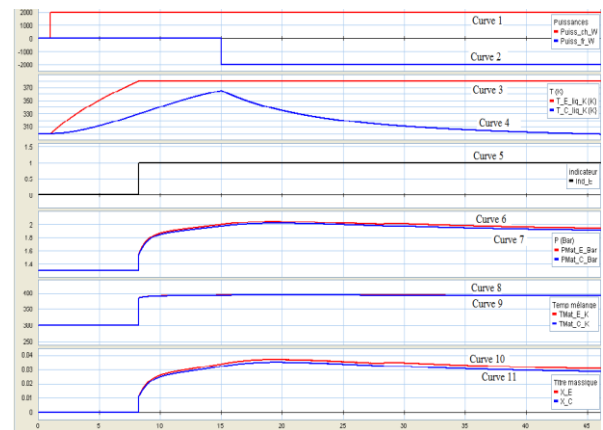


Fig. 14: Phase change in evaporator (red) and Condenser (Blue).

#### Analysis of the Figure 14:

The application of 2.0 kW (curve 1) at  $t=1s$  leads to a rise of fluid temperature within the evaporator and the condenser (Curve 3, 4). The evaporator temperature reaches the saturation value of water  $T=373K$  at  $t=7s$ . Curves 8 and 9 show the evolution of the mixture temperature in both

evaporator and condenser. The curve 5 shows the state indicator that displays the value 1 at the instant when the liquid temperature is: 373K. By switching from “0” to “1”, it informs about the moment of saturation, namely  $t = 7s$ . The fluid is now biphasic: liquid/vapor mixture, whose vapor quality is up to 0.3 %. Curve 10 (in evaporator) and curve 11 (in condenser). The curve 6 and 7 trace the evolution of the mixture pressure respectively in the evaporator and condenser. It is noted that once the cooling triggered at  $t = 15s$  (curve 2) the steam quality (curves 10 and 11) and the pressure (curve 6 and 7), start decreasing before stabilizing. The steam quality converges to an equilibrium value 0.2 %. Note that with a power  $P_{HS} = 2000 W$  and a flow rate  $q_m = 5 cm^3/s$ , the specific enthalpy can be calculated as given:  $\Delta h = \frac{P_{HS}}{q_m} = 2000/0.005 = 400kJ / Kg$ . According to Mollier diagram (P, H); theoretical corresponding steam quality would be 2%, a value which coincides well with the results available at the model output.

#### IV. CONCLUSION

The functioning principle of the cooling loops is based on the use of physical and thermodynamic properties of fluids. The concept of phase change and its efficiency in transferring energy was discussed. A second part is devoted to the presentation of a biphasic fluid loop model, in which the fluid is mechanically pumped. The modeling is based on Bond Graph approach. The third part includes the cases of simulation launched with the developed model. Note that this model is configurable, which means that it is possible to change, at any moment, the geometric conditions of the loop as well as the fluid properties. A test bench of the entire loop is under development, the purpose is validating the model in the short term with experimental results.

#### Variables

$C_p$	Specific heat	J/kg/K
$C$	Capacity	J/K
$h$	Specific enthalpy	J/kg
$h'$	Specific enthalpy of the liquid portion in the mixture	J/kg
$h''$	Specific enthalpy of the vapor portion in the mixture	J/kg
$H$	Enthalpy	J
$\dot{H}$	Heat flow	J/s
$L_v$	Latent heat	J/kg
$m$	Mass kg.	
$p_i$	with $i = 0, \dots, 6$ , Coefficients.	
$P$	Pressure Pa	
$q_m$	Mass flow	kg/s
$Q_{ap}$	Heat flow (Hot source)	J/s
$R$	Resistance.	
$T$	Temperature	K
$T_{sat}$	Saturation temperature	K
$v'$	Specific volume of the liquid in the mixture	$m^3/kg$
$v''$	Specific volume of the vapor in the mixture	$m^3/kg$
$v_{mel}$	Specific volume of the mixture	$m^3/kg$
$V$	Volume	$m^3$
$X$	Vapor quality.	
$u$	Internal specific energy	J/kg
$\rho$	Density of the fluid	$kg/m^3$
$v$	Velocity	m/s
$\eta$	Viscosity	Pa.s
$0$	Initial state.	
$liq$	Liquid.	
$evap$	Evaporator.	

<b>cond</b>	Condenser.
<b>m</b>	Mass.
<b>'</b>	Biphasic part of the evaporator.
<b>in</b>	Evaporator inlet.
<b>out</b>	Evaporator outlet.
<b>acc</b>	Accumulated.
<b>HS</b>	Hot source.
<b>CS</b>	Cold source.

#### ACKNOWLEDGMENT

This paper describes results from research supported by the FUI 14 Program in the context of project ThermoFluid RT labeled by the competitively pole ASTech. The authors gratefully acknowledge Mrs J. Duval and R. Albach from Atmostat Company for the multiple fruitful scientific discussions about innovative technologies.

#### REFERENCES

- [1] G. Dauphin-Tanguy, A. Rahmani, C. Sueur, “Bond graph aided design of controlled systems,” Simulation Practice and Theory, LAGIS: Laboratoire d’Automatique et d’informatique Industrielle de Lille, Ch.7, pp.493-513, 1999.
- [2] L. Lachasagne, “Numerical modeling and experimental development of a capillary pumped two-phase loop by gravity environment: application to the cooling of power electronic components in automotive context,” PhD thesis, National School of Mechanical and Aeronautical Engineering Poitiers, 2006.
- [3] K. Medjaher, AK. Samantaray, B. Ould Bouamama, “Bond Graph Model of a Vertical U-Tube Steam Condenser Coupled with a Heat Exchanger,” Article ELSEVIER, LAGIS: Laboratoire d’Automatique et d’informatique Industrielle de Lille, 2004.
- [4] A. Mukherjee, R. Karmakar, “Modeling and simulation of engineering systems through bond graphs,” Pangbourne, UK: Alpha Sciences International, 2000.
- [5] I. Muraoka, F.M Ramos, V.V Vlassov, “Experimental and theoretical investigation of a capillarity pumped loop with a porous element in the condenser,” Int. Comm. Heat Mass Transer, Vol.25, No 8, pp.1085-1094, 1998.
- [6] B. Ould Bouamama, K. Medjahera, A.K. Samantaray, M. Staroswiecki, “Supervision of an industrial steam generator. Part I: Bond graph modeling,” Article ELSEVIER. Control Engineering Practice, pp. 71–83, 2006.
- [7] B. Ould Bouamama, J.U. Thoma, J.P. Cassar, “Bond Graph modelisation of steam condenser,” Article IEEE, LAGIS: Laboratoire d’Automatique et d’informatique Industrielle de Lille, 1997.
- [8] V. Platell, C. Buttol, J.Y. Crandpeix, J.L. Joly, “Model Evaporator of two-phase fluid loop with capillary pumped,” Article IEEE , 1996.
- [9] E. Schmidt, “VDI tables constants steam,” 1963.
- [10] V. Serin, “Hydrodynamic and thermal study of the vaporization in a square section of micro channel: application to two-phase micro capillary pumped loops,” PhD thesis, University of Toulouse, 2007.
- [11] J.U. Thoma, “Introduction to bond graphs and their applications,” Oxford, New York: Pergamon Press, Systems dynamics: A unified approach, 2nd ed, New York: Wiley, 1975.
- [12] G. Wang, D. Mishkins, D. Nikanpour, “Capillary Heat Loop Technology: Space applications and recent Canadian activities,” VI Minsk International Seminar “Heat Pipes, Heat Pumps, Refrigerators”, 2005.